

Correlation between bow ice loads and operational responses during ice navigation in the Weddell Sea

Anriëtte Bekker¹, Liangliang Lu², Christof M. van Zijl¹, James-John Matthee¹ & Pentti Kujala²

¹ Sound and Vibration Research Group, Department of Mechanical and Mechatronic Engineering, (Stellenbosch University, Stellenbosch, South Africa).

²Marine Technology, Department of Mechanical Engineering, (Aalto University, Espoo, Finland).

ABSTRACT

In this era of digitalization, the increasing ability to analyze and display data in real-time, progressively enables monitoring services towards operational insight. In the light of this, full-scale measurements on the SA Agulhas II polar supply and research vessel were interrogated. These full-scale measurements comprise ice conditions, ice loads and structural vibration on the hull and propulsion system. The statistical distributions and underlying correlations between full-scale data and operational parameters are considered. Ice loads are measured with a permanent hull-installation. The correlation between ice load measurements and mobile accelerometer measurements is investigated in order to assess if hull measurements could be inferred at new hull locations. A correlation is shown between mobile acceleration sensors and ice loads at the bow, however, the correlation is not sufficient to allow for a conclusive prediction of ice loads from operational measurements. It is found that the first lateral bending mode is excited by ice passage. Furthermore, it is suggested that improved fidelity of ice condition data and the correlation of full-time histories may offer improved results.

KEY WORDS: Full-scale measurements; Ice loads; Vibration; Propulsion; Modal tracking; Ice load prediction.

INTRODUCTION

Questions pertaining to global warming marks the Weddell Sea in West Antarctica as an area of immense scientific interest owing to events in recent decades where the Larsen A, B and C ice shelves have broken from the continental mass. The Flotilla Foundation chartered the South African Polar Supply and Research Vessel, the SA Agulhas II in January 2019 to perform research in the Larsen B and C area and to hunt for the wreck of the Endurance, which was crushed by sea-ice during Sir Ernest Shackleton's trans-Antarctic expedition in the Weddell Sea. The vessel was the first to navigate in these waters since an expedition by the Polarstern in 2002.



Figure 1. SAA II vessel during offloading operations at Penguin Bukta, December 2018, Antarctica (Photo Credit: James-John Matthee).

The SA Agulhas II is owned by the South African Department of Environmental Affairs and has voyaged to Antarctica on annual relief voyages since 2012. She was equipped with full-scale instrumentation to measure hull ice loads, when she was manufactured by STX Finland in Rauma shipyard.

Table 1: Design limits for ice loading on SA Agulhas II hull.

	PC-5	DNV ICE 10
Stern	700 kN	790 kN
Bow	1150 kN	1650 kN

The SA Agulhas II is classified as a PC-5 vessel. However, her hull was maximally enforced to a hull classification of DNV ICE 10. For reference the design limit values for ice class PC-5 and DNV ICE 10 are listed in Table 1. Such hull measurements provide insight as to operational loading of an ice-going ship in the Antarctic environment. The full-scale instrumentation of the SA Agulhas II has expanded significantly through an active research program between Aalto University and Stellenbosch University. This research program has generated an expansive set of operational data.

However, the intent is not to drown in data, but to derive insight from this slumbering asset

(Bekker *et al.*, 2018). The growing demand for predictive capacity spurs the need to pair live data from on-board sensor networks with modelling capability in powerful digital twin platforms of the future. As ever, the cost of such services in terms of sensor infrastructure, data storage and analytical capacity will be offset against the potential business value of such services. Measurements and data analytics can be combined to deliver a system for real-time ice load monitoring. Presently the starboard side of the ship hull is instrumented for ice load monitoring, through a visionary effort during her construction phase. The question is if loading on the port side hull could be inferred through the use of a sensor installation post-manufacturing? This work proposes to explore the underlying correlations between ice loads and other relevant full-scale measurements to address the following aspects:

1. Can accelerometers, that track bending modes, be used to predict ice loading at the bow?
2. Can ice loading on the hull be predicted through a regression model of other full-scale measurement variables?

MEASUREMENT SETUP AND EQUIPMENT

Table 2. Full-scale ship-based measurement instrumentation on the SA Agulhas II.

Measurement	Variables	Equipment	Number of channels	Sample rate
Ship context	Camera footage	Bosch underway camera system	~40	1 Hz
Wave	Height, direction	Visual observations	1	4 hours
Sea Ice	Thickness, ice cover, floe size	GPS	2	1 Hz
		Underway top camera - floe size, ice concentration	2	0.5 Hz
		Underway stereo camera – ice thickness	2	3 Hz
		Visual observations (Concentration, floe size, thickness)	3	10 Min
Ship vibration response (hull and super-structure)	Acceleration (Rigid body motion and flexure)	DC accelerometers,	10	2048 Hz
		ICP accelerometers	20	2048 Hz
Ship - shaft-line torsional and thrust vibration	Thrust, Torque,	Strain gauges, V-links and Quantum data acquisition units	2	600 Hz
	Bearing acceleration	Accelerometers to Quantum data acquisition units	6	2048 Hz
Ship - hull ice loading	Bow, bow shoulder and stern shoulder loads	Strain gauges, Central measurement unit	56 (+ 9)	200 Hz
Ship – AIS data	Various sensors and ship central measurement unit	Time, latitude, longitude, SOG, COG, HDT, relative wind direction, wind speed, depth	9	1 Hz
Ship machine control		Propeller motor current, speed and voltage for starboard propeller. Rudder order, position and pitch for port- and starboard shaft, rpm.	26	0.5 Hz
Ship rigid body motion	Inertial measurement units (IMU)	yaw, pitch, roll, heave, surge, sway	2	1 Hz

Full-scale measurements on the Weddell Sea Expedition 2019 include almost 200 measurement channels (Table 2) and comprise measurements of hull-loading, global vibration responses, indirect measurements of torque and thrust (portside shaft), operational ship parameters and context and finally, subjective observations of ice conditions and wave height. Details of the individual measurement rigs are described by (Bekker *et al.*, 2018).

TRANSIT DESCRIPTION

Table 3. The Captain's log of the transit from Thimbul ice shelf to the Western Weddel Sea

Date	Time	Operating Mode	Vessel Activity
1 Jan	00:00	DP	Stationary off Otter Bukta.
	11:36	Sea-Mode	Transit to bay ice.
	12:06	Sea-Mode	Stationary, bow to bay ice.
	19:09	DP	Station AM000969.
	19:24	Sea-Mode	Stationary, bow to bay ice.
2 Jan	15:30	Sea-Mode	Backing off from bay ice.
	16:08	DP	Station AM000970.
	18:06	Off DP, Sea-Mode	-
	18:18	DP	-
	18:54	Off DP, Sea-Mode	-
	19:06	DP	-
	19:42	Off DP, Sea-Mode	-
	20:00	DP	-
	21:37	Off DP, Sea-Mode	Transit to Penguin Bukta.
3 Jan	00:18	DP	Stationary off Penguin Bukta discharge site.
	11:39	Off DP, Sea-Mode	Transit to discharge position at ice shelf.
	12:18	Sea-Mode	Bow to ice shelf.
	13:54	Sea-Mode	Backing off from ice shelf.
	14:06	Sea-Mode	Drone recovery from ice shelf.
	14:54	Sea-Mode	Transit to Larsen C.
4 Jan	13:24	Ice-Mode	Transit to Larsen C.
6 Jan	13:00	Sea-Mode, constant rpm	Transit to Larsen C.
9 Jan	01:24	DP	Station AM000972.
	04:00	Sea-Mode	Transit to next station.
	05:30	DP	Station AM000973.
	07:12	Off DP, Sea-Mode	Transit to next station.
	14:00	DP	Station AM000974.
	15:42	Sea-Mode	Transit NW to Larsen C.
10 Jan	21:15	DP	Station AM000975.
	23:19	Sea-Mode	Transit to Larsen C.

Table 3 provides information from the Captain's log book relating to vessel activities from 1 to 10 January and the operating mode of the vessel during these activities. From 1 to 3 January the vessel maintained position close to the logistics discharge point on the ice shelf at Penguin Bukta. Transit from Penguin Bukta to Larsen C started at 14:54 on 3 January. During transit the vessel operated mostly in sea-going mode. However, from 13:24 on 4 January to 13:00 on 6 January operations were switched to ice-mode. On 9 January three scientific stations were conducted in the region surrounding Larsen C and the vessel was stationary in DP (Dynamic Positioning) mode for the duration of the stations. Between stations, the aim was to navigate as rapidly as possible, within allowable safety limits. The navigational strategy avoided ice whenever possible and opted for open water leads in floe fields. Ship speed was reduced as required for safe ship navigation in misty or icy conditions.

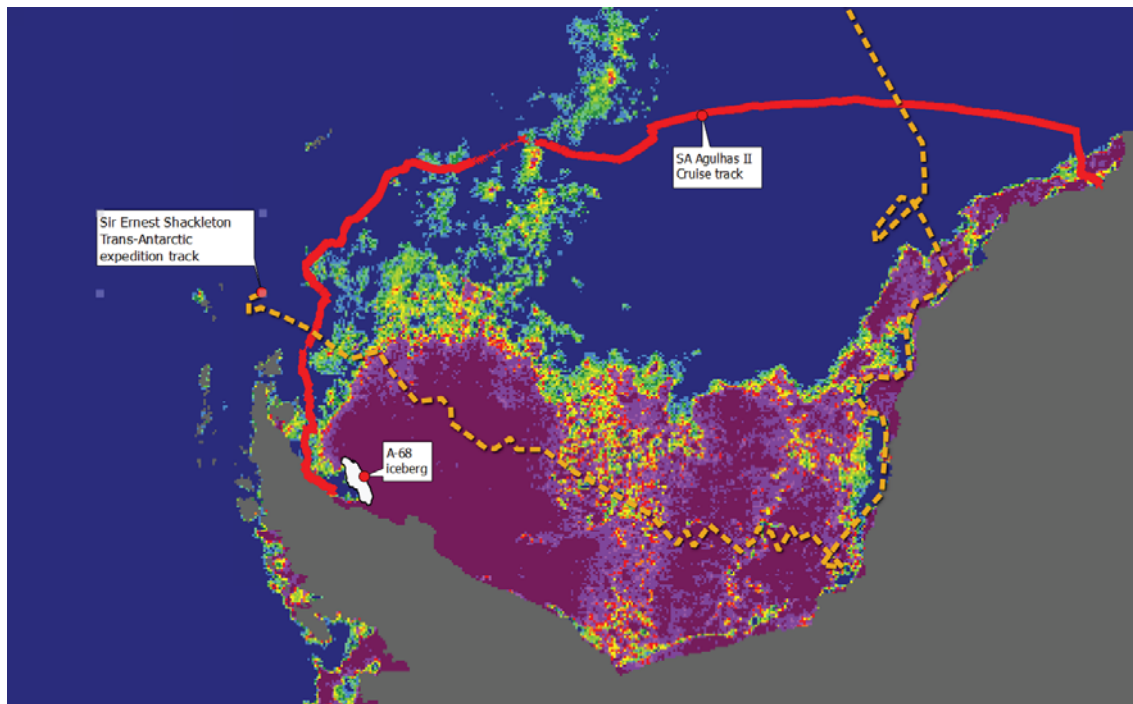


Figure 2. The SA Agulhas II cruise track from 3 to 10 January between Penguin Bukta and the Larsen C Ice Shelf.

RESULTS

Ice conditions

Ice conditions were determined through visual observations on the Bridge in round-the-clock surveillance shifts when the vessel engages in ice-passage as shown in Figure 3. A yardstick with 10 cm long black and white markings is suspended over the edge of the ship. As the ice rotates upwards alongside the hull the observer is tasked to judge for how many minutes in a 10 minute interval a certain ice thickness was experienced (Suominen *et al.*, 2017; Bekker *et al.*, 2018). On the present transit the vessel encountered mostly first year ice of up to 1.5 m thick in ice concentrations ranging from open water to fully consolidated ice. Floes ranged from a few meters to over a kilometer in dimension. Observers were tasked to classify floe size into the following categories: <20 m (narrower than ship width); 20 to 100 m (shorter than the ship length); 100 to 500 m; 500 to 2000 m; 2000 to 5000 m and 5000+ m. Observations are recorded every 10 minutes as estimates of ice thickness, floe size and ice concentration as presented in Figure 4. During transit, observers continually note their observations every minute. Ten minute estimates are subsequently calculated by determining the average ice thickness, floe size and ice concentration over the observed time. The present data comprise the surveillance of four observers who worked on 3 hour shifts during the transit.

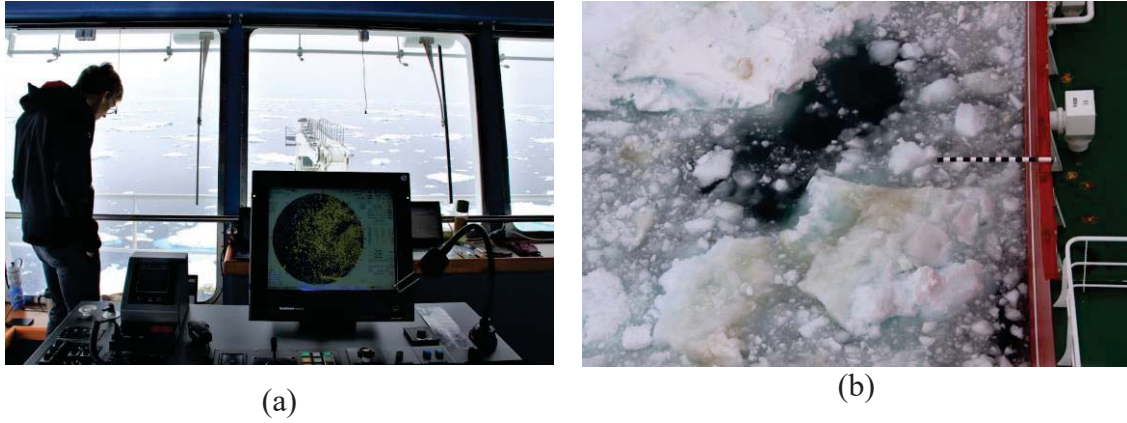


Figure 3. (a) An observer on the bridge uses a (b) yardstick, suspended from the port side of the ship to estimate the thickness of over-turning ice as the vessel navigates through ice.

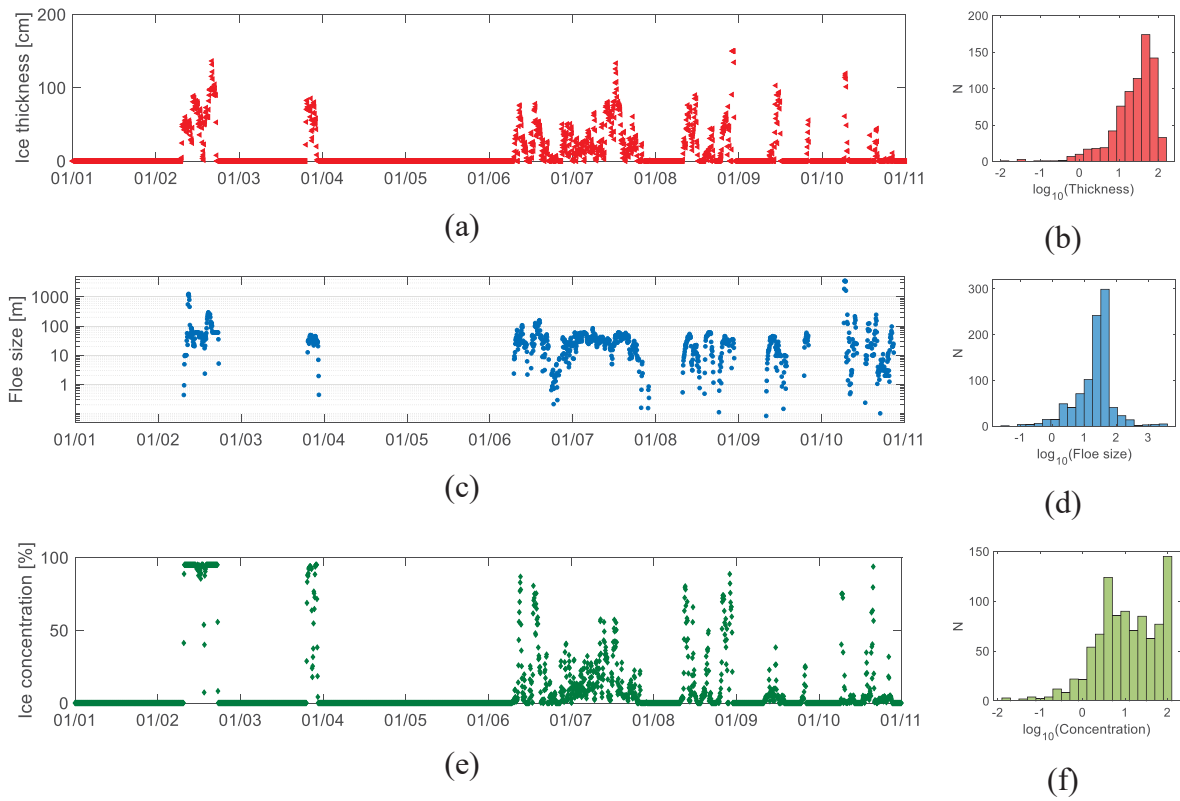


Figure 4 Visual observations and distributions of (a & b) ice thickness, (c & d) floe size and (e & f) ice concentration.

Propulsion measurements

Operational torque was recorded using strain gauge bridges on the port-side shaft of the SA Agulhas II. The reported mean values are intended to reflect the low frequency changes in thrust and torque values which are dictated by the power demand from the ship controls. The amplitude values reflect the difference between the peak torque or thrust and the average values.

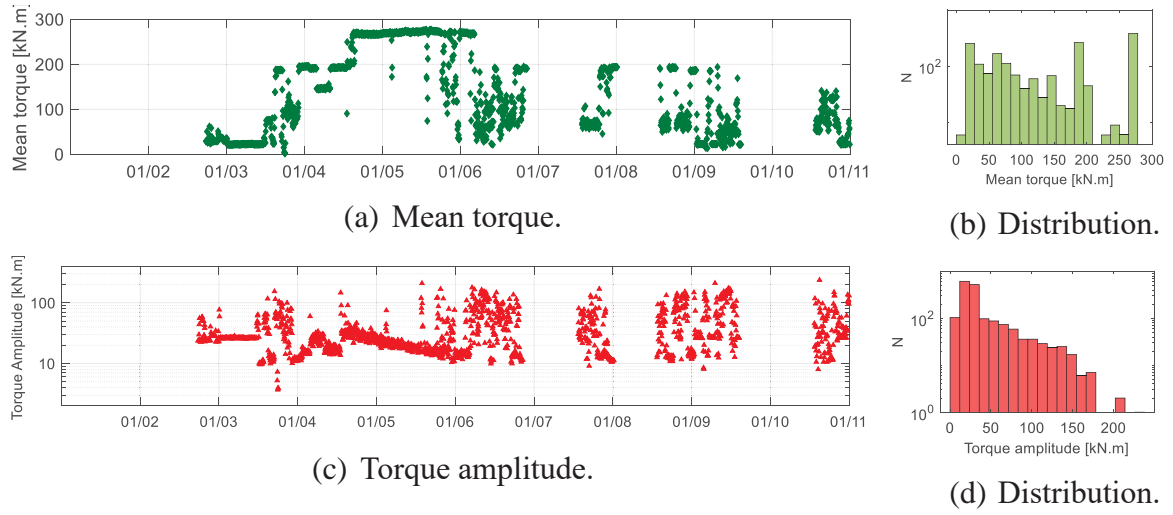


Figure 5: Five-minute metrics as calculated from measurements on the port-side shaft.

AIS data

From 1 to 10 January, navigation of the SA Agulhas II was focused on spending the minimal time in transit between scientific stations. An operational profile of the transit was generated through combined consideration of full-scale data, research notes and navigational logs. Operations were classified as ice navigation when the ice concentration $> 0\%$ according to visual observations. At vessel speeds < 0.5 kn it was assumed that the ship was operating on station in DP mode. According to these assumptions the transit comprises 40% open water navigation, 33% ice navigation and 27% on station.

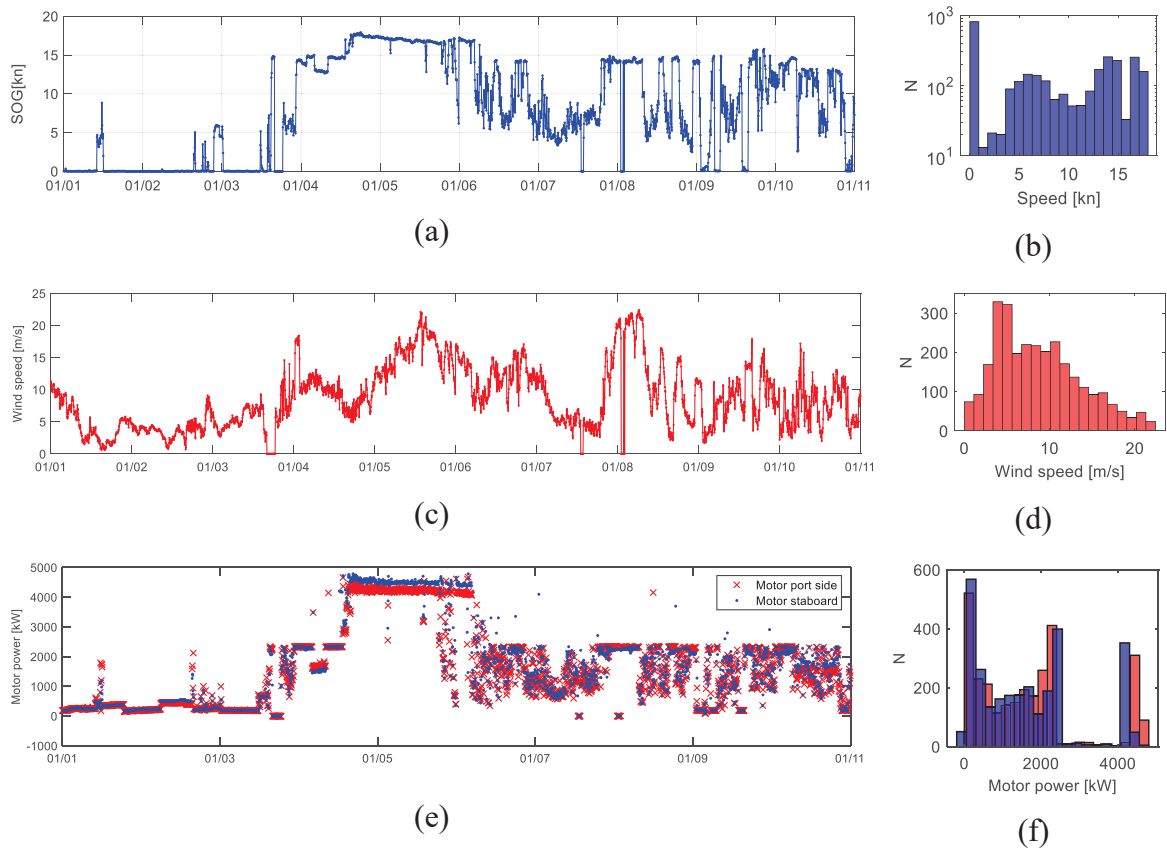


Figure 6. The time traces and distributions of (a & b) SOG, (c & d) wind speed and (e & f) motor power.

Vibration measurements

Five-minute peak values were calculated from full-scale vibration measurements in locations close to the ice load measurements. The peak values are presented in Figure 7 for measurement locations in the bow chain lockers, forward cargo hold and steering gear room, with the intent to correlate these measurements with ice loads at the bow, bow shoulder and stern shoulder.

Note that the measurement system was started on 2 January at 18:15. There are segments with missing data because of power losses to the DAQ in the steering gear room during voyage safety drills. The most noticeable was between 3 and 4 January. The system was fully functional from 4 January at 13:26.

As expected, peak acceleration values recorded at the bow and stern of the vessel were higher during ice navigation than open water navigation. Peak acceleration values were the highest at the bow and stern and significantly lower at the bow shoulder. The maximum five-minute peak acceleration occurred at both the bow and stern between 00:50 and 00:55 on 7 January. During this time the vessel was navigating through loosely packed ice (thirty to forty percent ice concentration, average floe size 20 m in diameter and average ice thickness between 60 and 70 cm) at approximately 3 knots in sea-going mode.

Modal analysis

The possible refinement of vibration data was considered by extracting operational vibration modes from the global vibration response of the vessel using operational modal analysis (OMA) (Soal, 2018). A combination of in-house and open source algorithms was implemented to identify global modes of vibration and to track changes in modal parameters over time.

The frequency domain decomposition (FDD) technique was used to perform OMA. FDD involves performing a singular value decomposition on the spectral density matrix of output measurements at discrete frequency lines. The spectrum of singular values contains peaks at frequencies that correspond to the natural frequencies of the test structure. The singular vectors that correspond to the singular values are estimates of the mode shapes. A variation of the FDD technique known as enhanced FDD (EFDD) further provides damping estimates. Damping ratios are determined by performing an Inverse Fast Fourier Transform (IFFT) of the spectral density matrix in a user-specified band of frequency lines surrounding a single identified mode. The resulting correlation function is an estimate of a free decay of a single degree of freedom system and damping ratios are calculated from the logarithmic decrement of the free decay. An enhanced estimate of the damped natural frequency is calculated from the number of zero crossings of the free decay. Figure 8(a) presents an example of the spectrum of singular values of the spectral density matrix calculated from twenty minutes of measured data. Several modal peaks may be identified from this set of singular values. For each identified modal peak, mode shapes and damping ratios may be estimated according to the methods described above.

An automatic modal selection algorithm based on the EFDD technique was developed to process data from 1 to 10 January. Modes were selected from a spectrum of singular values using the MATLAB `findpeaks()` function. Subsequently, mode shapes and damping ratios were calculated for each of the identified modes. This was applied to twenty-minute segments of data with 75 percent overlap between subsequent segments.

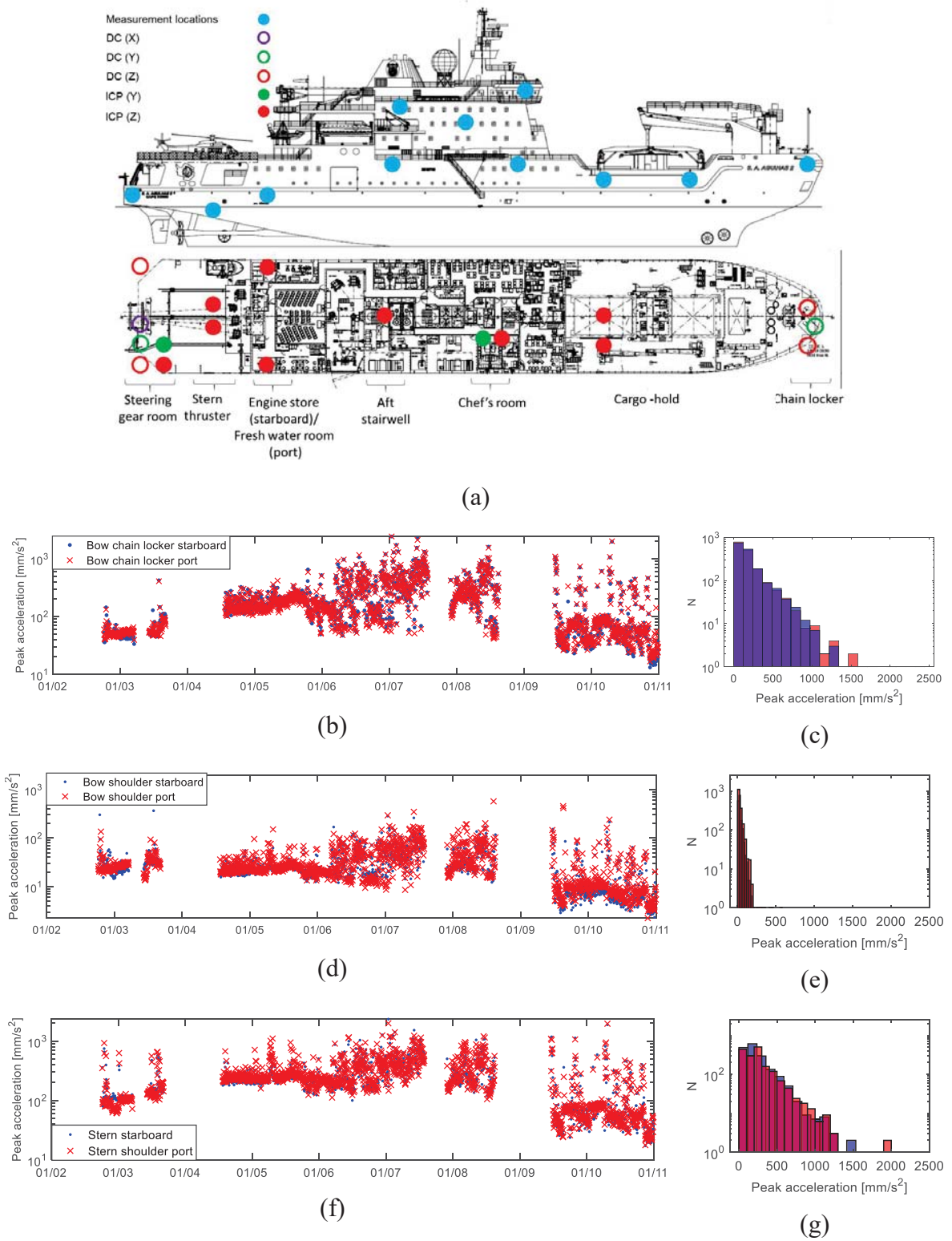
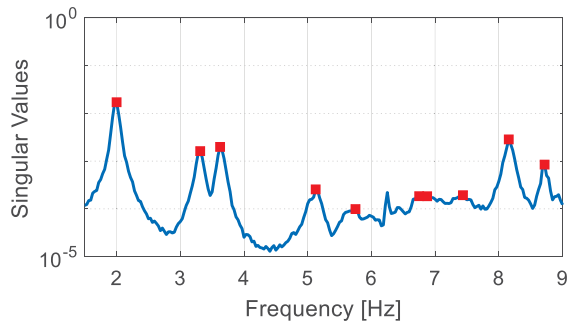
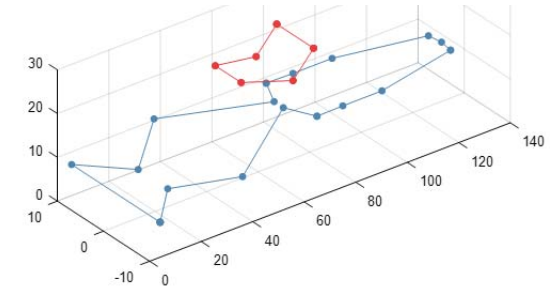


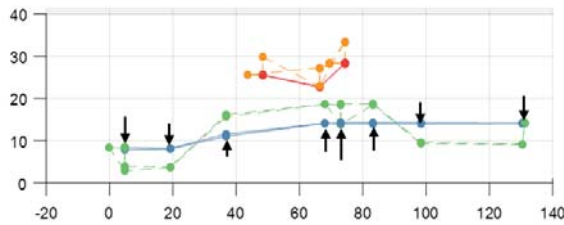
Figure 7: (a) An overview of the full-scale accelerometer setup and selected measurement locations. Five-minute, vertical, peak acceleration and distribution of structural vibration at the (b & c) bow chain locker, (d & e) bow shoulder cargo-hold and (f & g) steering gear room.



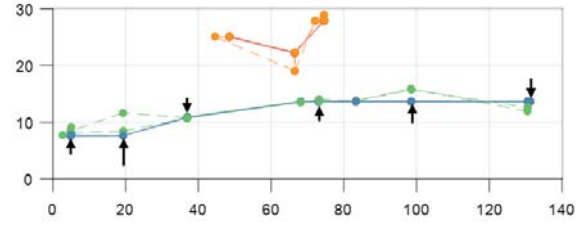
(a) Singular value decomposition of vibration data.



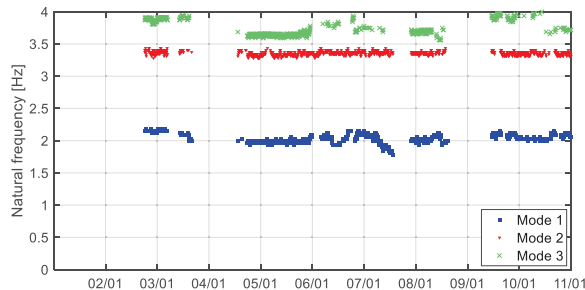
(b) Original discretized geometry of SA Agulhas II.



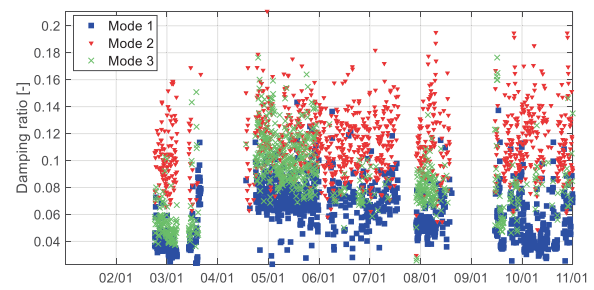
(c) Mode 1: First vertical bending



(d) Mode 3: Second vertical bending



(e) Frequency tracking for first three modes.



(f) Damping tracking for first three modes.

Figure 8: Operational modal analysis and modal tracking for 1 to 10 January.

Three modes with natural frequencies at approximately 2.0 Hz, 3.4 Hz and 3.7 Hz were tracked over the transit duration and represent the first vertical bending, first lateral bending and second vertical bending modes of the vessel hull.

Measurement system offline for parts of 1,2,3,8 and 9 January. No modes are identified here. On 2 and 3 January there were long periods when the vessel was stationary (parked bow to bay ice at Otter Bukta). All three modes appear to be well-excited and are tracked successfully.

From 4 to 9 January the vessel was in transit from Penguin Bukta to Larsen C. There were times on 6 and 7 January when the two vertical bending modes (Mode 1 and Mode 3) were not identified. Notably this occurs when the vessel was operating in ice conditions and the speed was relatively low and varying. During this time the lateral bending mode was well excited. During this time the vessel was navigating in generally loosely packed ice and there were occasional impacts with ice floes which redirected the heading of the ship. It is possible that this excites lateral modes of the ship. In these conditions the sea-state is fairly calm so there would be little excitation in the vertical direction.

The natural frequencies of modes are generally lower when the vessel was moving compared to when it was stationary. This is particularly noticeable for Mode 3. The damping ratios of modes are generally higher when the vessel was moving compared to when it was stationary. In addition to not being well excited during ice navigation, Mode 1 and 3 also appear to have higher natural frequencies during ice navigation than in open water. May be due to lower speeds. Mode 2 has a relatively constant natural frequency.

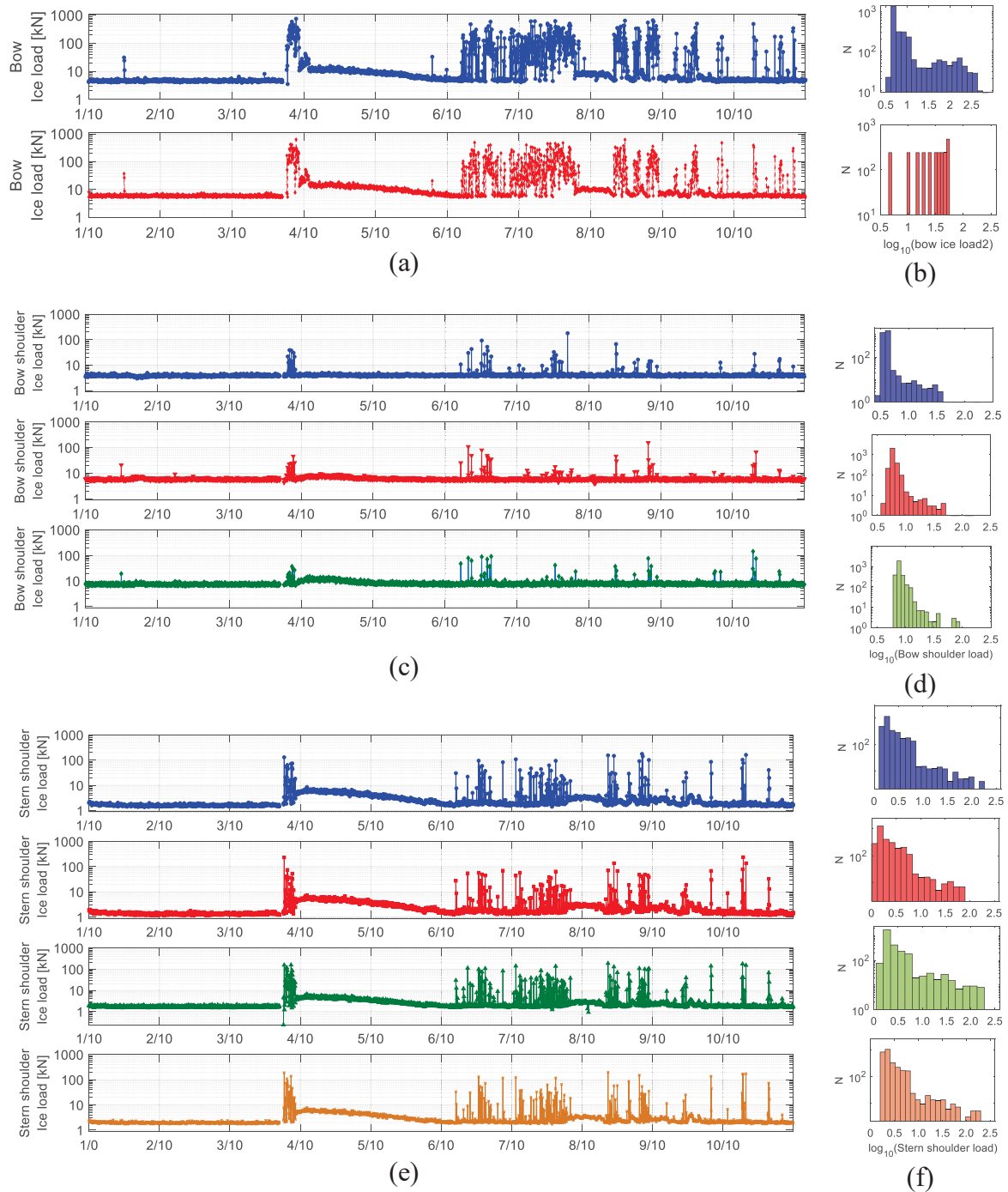


Figure 9: The time traces and distributions of five-minute maxima of ice loads at the (a & b) bow, (c & d) bow shoulder and (e & f) stern shoulder.

Ice load measurements

The strain gauge measurements measure shear strain responses in the upper and lower sections of the instrumented hull frames. The data were organized in five-minute sample records and referenced to UTC time. The ice loads (shear force) are determined through an in-house algorithm based on Raleigh separation (Kotilainen *et al.*, 2017). Five minute maximum ice loads were calculated as shown in Figure 9.

It is observed that ice loads are mostly registered at the ship bow sensors for the transit between Thimbul Ice Shelf and the western Weddell Sea. This is expected as the bow is mainly breaking and paving ice when the ship encounters pack ice. During transit, when the ship bow has paved

the ice away, ice impacts on the other parts of the hull are relatively low.

Ice loads occurred from late afternoon on January 3rd and reached a peak value of 834 kN at the bow, which corresponds to a period when the ship is paving ice and leaving from Penguin Bukta to Weddell Sea. The next period of consistent ice loading is from January 6th morning to January 8th night, when the ship reached the western Weddell Sea. In this time several ice loads exceeded 600 kN. The last period of relatively constant ice impact on ship is from January 8th morning to 9th, reaching around 650 kN and after that, there was little constant dense ice conditions and ice loads.

A preliminary statistical investigation of the ice loads shows that the ice loads for two frames at the bow are statistically significantly different. The same was concluded for the three measurements at the bow shoulder and four measurements at the stern shoulder. The data from all sensors are non-normal and right-skewed.

Correlation

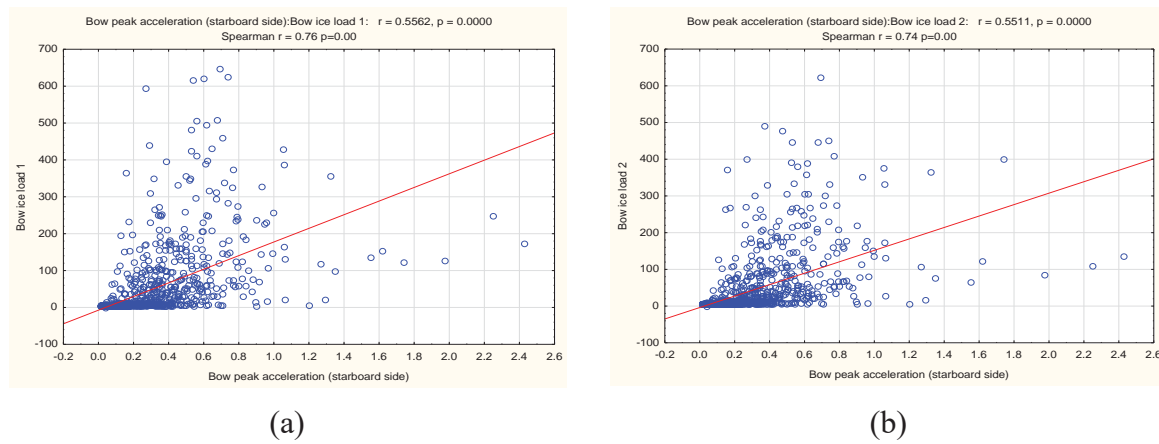


Figure 10. Correlation plots between (a) the starboard side chain locker peak acceleration and peak ice loads at frame 1 and (b) the starboard side chain locker peak acceleration and the peak ice loads at bow frame 2.

The starboard hull frames of the SA Agulhas II were equipped with strain gauges for ice load measurements when she was manufactured in Rauma shipyard. The question arises if it is possible to attain such measurements on the portside hull through retrospectively added sensors, such as accelerometers. The correlation plots in Figure 10 show that peak acceleration values at the bow chain lockers are correlated with peak ice loads at the bow. The correlation is not conclusive (spearman $R = 0.76$ and $R = 0.74$ respectively) and the many outliers indicate that other factors account for the variation in both vibration and ice loads.

Regression analysis to predict bow ice load

As the transit under investigation mostly resulted in elevated bow loads, regression models were investigated to model Bow ice load 1 ($F_{bow,1}$) through a combination of other operational measurements. The most promising regression model ($R = 0.52$) involved the combination of floe size (S_{floe}), ice thickness (T_{ice}), ice concentration (C_{ice}), SOG and propulsion motor power (P) as follows:

$$\log_{10}(F_{bow,1}) = b_1 S_{floe} + b_2 T_{ice} + b_3 C_{ice} + b_4 SOG + b_5 P_{port} + b_6 P_{stb} \quad (1)$$

The regression parameters are listed in Table 4. The parameters considered in this model are sensical as they all conceivably correlate with ice load. However, closer scrutiny of the parameters raises several questions about the fidelity of the presented model. This includes negatively correlated ice concentration, floe size and SOG which are expected to correlate

positively. This non-sensical result does point to the dangers of the blind use of data for models and possible re-consideration of the veracity or suitability of data used for regression analysis.

Table 4: A regression analysis for the prediction of bow ice load 1 ($F_{bow,1}$).

	Regression Summary for Dependent Variable: log10(Bow ice load 1) (Spreadsheet58) R= .52427					
	b*	Std.Err. of b*	b	Std.Err. of b	t(947)	p-value
N=954						
Intercept			1.257063	0.06887	18.25276	0
Floe size	-0.13977	0.028812	-0.000334	0.000069	-4.85103	0.000001
Ice thickness	0.411267	0.041726	0.008571	0.00087	9.85628	0
Ice concentration	-0.395099	0.045051	-0.007834	0.000893	-8.77001	0
SOG	-0.44029	0.050608	-0.074719	0.008588	-8.69995	0
Propulsion motor power (port side)	0.23716	0.061617	0.000253	0.000066	3.84894	0.000127
Propulsion motor power (starboard side)	0.229406	0.062021	0.000234	0.000063	3.69881	0.000229

Figure 11 shows a box and whisker plot as a result of multi-variate data combinations according to terminal groupings. Notably the second terminal grouping presents a lot of high outlier loads at meagre ice concentrations. This is potentially explained by the fact that ten minute average ice concentrations are reported. As such a high ice load could occur if a high ice concentration was present for only a fraction of the ten-minute observation window.

Figure 12 sheds light on the fact that not all ice load terminal groupings can be determined with equal confidence. As an example, only nine data cases are present to confirm the maximal ice load observations during the western transit to the Weddell Sea. This points to the possible need for more data of higher bow loads to increase model fidelity.

DISCUSSION

The SA Agulhas II operated at superior speed when the vessel was engaged in ice mode for open water navigation from 4 to 6 January. At this time the propulsion motors generated in the region of 4500 kW power to reach speeds in the region of 18 kn. In this time the mean torque varied around 280 kN.m, 40% more than in sea mode. The maximal excitation from the propulsion plant leads to excitation of the entire vessel structure, which is evident in the shaft torque, vibration measurements and shear strain measurements (ice load measurements) in the hull.

The correlation of peak ice loads and peak vertical vibration at the ship bow is not conclusive enough to result in a satisfactory model through which ice loads can be inferred from vibration measurements. It is considered that a correlation has been attempted using reduced data (five-minute peak values) and not detailed time traces. It is proposed that a more detailed correlation study could be performed whereby strain history at the bow is correlated with vertical acceleration at the bow chain locker. Consideration of the modal analysis shows that the bending modes or not well-excited during ice passage. As such ice load predictions using lateral acceleration sensors could be considered as a superior alternative for ice load correlation.

A regression analysis, to predict ice loads from other observed variables, is not successful. One comment is that peak ice loads were correlated to ten-minute averages values from visual observations. As an example, if an ice thickness of 1 m was observed for 1 min (out of 10 minutes) and the rest of the transit was in open water, the mean ice thickness would be 0.1 m. The peak ice load in this time is more likely to correlated with the maximum observed ice thickness, ice concentration and floe size. Furthermore, data from individual observers is susceptible to observer variability, lapses in concentration and individual bias. The quality of ice condition data could likely be improved by the objective measurement of ice conditions through camera vision.

The histograms of operational data point to the fact that more observations are available for certain ranges of operational variables. This implies that models of ice loads can be fitted with variable certainty, based on the amount of training data available, As such it could be beneficial

to include more data in the training data set.

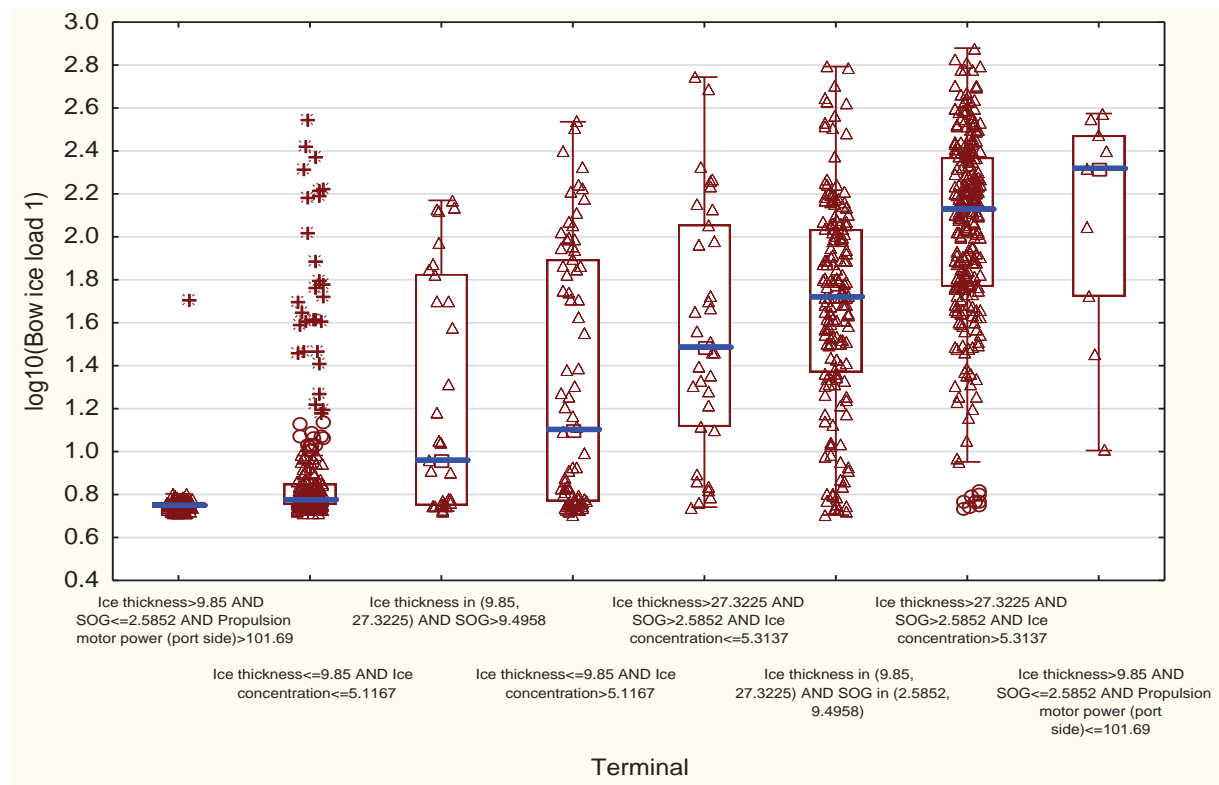


Figure 11: Box plots showing the scatter of observed ice loads according to terminal groupings in terms of variables including ice thickness, propulsion power, ice concentration and SOG.

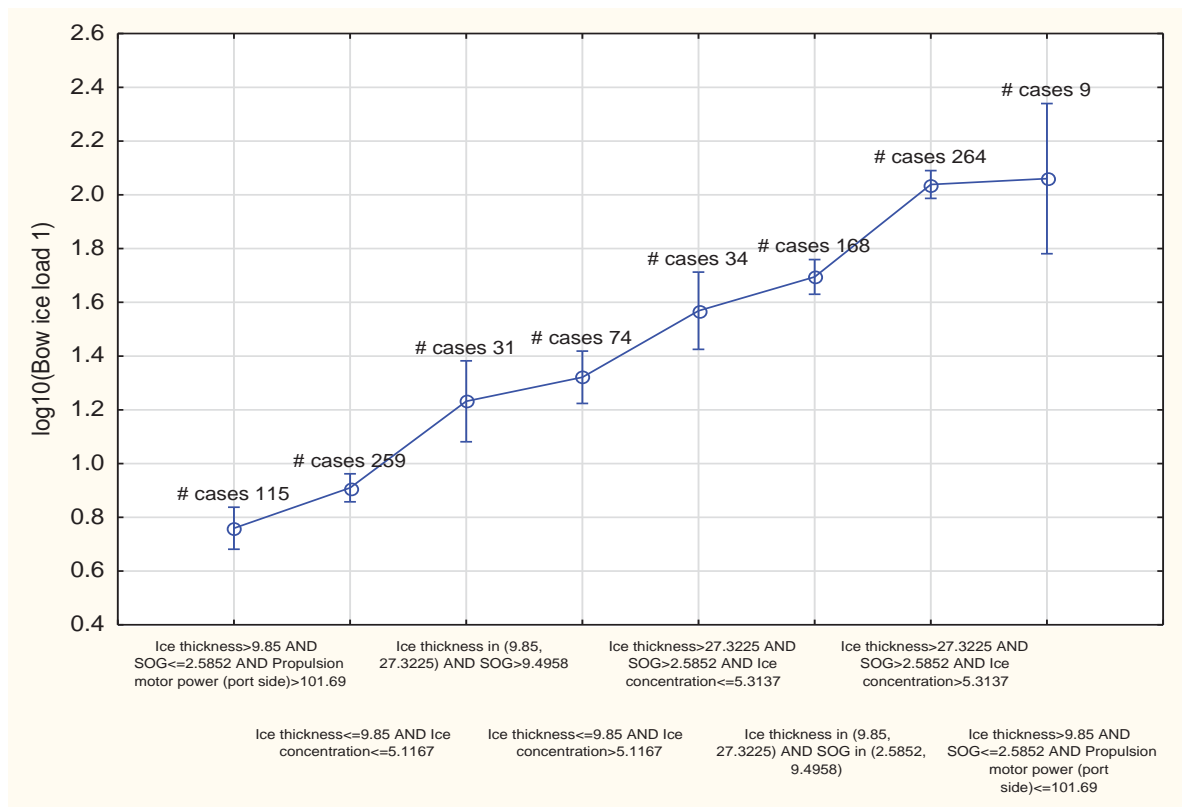


Figure 12: Information on the available training data in terminal groupings of the data set.

CONCLUSIONS

The present approach was not successful in achieving a near complete correlation between bow acceleration loads and peak ice loads from bow measurements. The best regression model, using operational data includes physically counter-intuitive variable combinations. Further interrogation of the regression model shows that five-minute maxima of ice loads should potentially be correlated with maxima of observed ice conditions. The option of higher fidelity ice condition data should be considered along with more data of extreme ice loading conditions on the hull.

ACKNOWLEDGEMENTS

The Flotilla Foundation is acknowledged for funding the charter of the SA Agulhas II for the Weddell Sea Expedition, 2019. The authors express thanks to the Department of Environmental Affairs and Captain Knowledge Bengu and Crew of the S.A. Agulhas II for their support and assistance during the Weddell Sea Expedition 2019. Funding from the National Research Foundation (NRF) through the South African National Antarctic Programme (SANAP Grant No.110737) is thankfully recognized.

REFERENCES

- Bekker, A. *et al.* (2018) 'From data to insight for a polar supply and research vessel', *Ship Technology Research*, pp. 1–34.
- Kotilainen, M. *et al.* (2017) 'Predicting ice-induced load amplitudes on ship bow conditional on ice thickness and ship speed in the Baltic Sea', *Cold Regions Science and Technology*. Elsevier B.V., 135, pp. 116–126. doi: 10.1016/j.coldregions.2016.12.006.
- Soal, K. (2018) *System identification and modal tracking of ship structures*. Stellenbosch University.
- Suominen, M. *et al.* (2017) 'Visual Antarctic Sea Ice Condition Observations during Austral Summers 2012-2016', in *Port and ocean Engineering under Arctic Conditions*. Busan, Korea.